



HAL
open science

Hyaluronic acid-conjugated liposomes loaded with dexamethasone: A promising approach for the treatment of inflammatory diseases

Kamila Bohne Japiassu, Francois Fay, Alessandro Marengo, Sebastião A Mendanha, Catherine Cailleau, Younès Louaguenouni, Qinglin Wang, Stéphanie Denis, Nicolas Tsapis, Thais Leite Nascimento, et al.

► To cite this version:

Kamila Bohne Japiassu, Francois Fay, Alessandro Marengo, Sebastião A Mendanha, Catherine Cailleau, et al.. Hyaluronic acid-conjugated liposomes loaded with dexamethasone: A promising approach for the treatment of inflammatory diseases. *International Journal of Pharmaceutics*, 2023, 639, pp.122946. 10.1016/j.ijpharm.2023.122946 . hal-04173093

HAL Id: hal-04173093

<https://hal.science/hal-04173093>

Submitted on 28 Jul 2023

HAL is a multi-disciplinary open access archive for the deposit and dissemination of scientific research documents, whether they are published or not. The documents may come from teaching and research institutions in France or abroad, or from public or private research centers.

L'archive ouverte pluridisciplinaire **HAL**, est destinée au dépôt et à la diffusion de documents scientifiques de niveau recherche, publiés ou non, émanant des établissements d'enseignement et de recherche français ou étrangers, des laboratoires publics ou privés.

Hyaluronic acid-conjugated liposomes loaded with dexamethasone: a promising approach for the treatment of inflammatory diseases

Kamila B.Japiassu^{a,b}, Francois Fay^a, Alessandro Marengo^a, Sebastião A. Mendanha^b, Catherine Cailleau^a, Younès Louaguenouni^a, Qinglin Wang^a, Stéphanie Denis^a, Nicolas Tsapis^a, Thais L. Nascimento^b, Eliana M. Lima^b and Elias Fattal^{a}*

^a Université Paris-Saclay, CNRS, Institut Galien Paris-Saclay, 91400 Orsay, France. *e-mail: elias.fattal@universite-paris-saclay.fr

^b Center for RD&I in Pharmaceutical Nano/Technology (FarmaTec), Federal University of Goiás, Goiania, 74605-220 Goiás, Brazil.

Abstract

Dexamethasone is a well-known anti-inflammatory drug readily used to treat many lung diseases. However, its side effects and poor lower airway deposition and retention are significant limitations to its usage. In this work, we developed lipid nanoparticulate platforms loaded with dexamethasone and evaluated their behavior in inflammatory lung models *in vitro* and *in vivo*. Dexamethasone-loaded liposomes with an average diameter below 150 nm were obtained using a solvent injection method. Three different formulations were produced with a distinct surface coating (polyethylene glycol, hyaluronic acid, or a mixture of both) as innovative strategies to cross the pulmonary mucus layer and/or target CD44 expressed on alveolar proinflammatory macrophages. Interestingly, while electron paramagnetic spectroscopy showed that surface modifications did not induce any molecular changes in the liposomal membrane, drug loading analysis revealed that adding the hyaluronic acid in the bilayer led to a decrease of dexamethasone loading (from 3.0 to 1.7w/w%). *In vitro* experiments on LPS-activated macrophages demonstrated that the encapsulation of dexamethasone in liposomes, particularly in HA-bearing ones, improved its anti-inflammatory efficacy compared to the free drug. Subsequently, *in vivo* data revealed that while intratracheal administration of free dexamethasone led to an important inter-animals variation of efficacy, dexamethasone-loaded liposomes showed an improved consistency within the results. Our data indicate that encapsulating dexamethasone into lipid nanoparticles is a potent strategy to improve its efficacy after lung delivery.

Key-words: dexamethasone; liposomes; inhalation; CD44 receptor; inflammation

1. Introduction

Dexamethasone (Dex) is a corticosteroid that exerts potent anti-inflammatory and immunosuppressive effects and is currently part of the World Health Organization's list of essential medicines (World Health Organization, 2021). Due to its anti-inflammatory ability, Dex has been extensively used in treating a wide range of inflammatory pulmonary diseases such as asthma, acute lung injury, COPD, acute respiratory distress syndrome, and COVID-19 (Rhen and Cidlowski, 2005; Noreen et al., 2021).

Although Dex is affordable and widely available, its systemic administration over a long period can cause many side effects, such as muscle weakness, bone loss, cataracts, and candidiasis (Saag et al., 1994; McDonough et al., 2008). Thus, despite the potential therapeutic effect of Dex, its prolonged use remains a serious concern (García-Fernández et al., 2021). In the past decades, local lung administration of corticosteroids by inhalation for treating pulmonary conditions was shown to be highly efficient and associated with optimal patient tolerance. In addition, inhaled corticosteroids allow for a rapid onset of action and induce fewer side effects than administration by other routes (Matthieu et al., 2014). Pulmonary delivery also enables a relatively uniform drug distribution in the lower airways and avoids hepatic first-pass metabolism, increasing the local availability of the drugs. Thus, inhalation of corticosteroids offers many advantages over the administration by the systemic route to treat conditions that require either high doses or repeated administration of the drug (Daley-Yates, 2015).

Despite significant signs of progress in this area, inhalation therapies still need innovations to expand their uses and applications (Schneider et al., 2017). Major limitations concern the moderate deposition of drugs in the lower airways, the toxicity in healthy lung tissues, and the limited lung retention time (Lai et al., 2009; Almeida et al., 2019). Indeed, Dex is water insoluble, and this property represents a considerable challenge in developing

nebulization-based strategies since, after a short passage in the lungs, the drug is rapidly absorbed into the blood (N'Guessan et al., 2017). Therefore, Dex pulmonary administration in lung inflammatory diseases by nanostructured carriers represents a promising strategy due to the high uptake of these carriers by phagocytic immune cells (Blank et al., 2017).

Several past studies, including ours, have shown the benefits of using liposomes and other nanoparticles displaying poly(ethylene glycol) (PEG) and hyaluronic acid (HA) on their surface as strategies to improve respectively mucus penetration and alveolar macrophages (AM) targeting through HA interaction with CD44 expressed on AM cell membrane (Wang et al., 2008; Kelly et al., 2011; Suk et al., 2016; Ponzoni et al., 2018; Pandolfi et al., 2019). AM are one of the key cellular components of the dysregulated inflammatory response during acute lung injury. Therefore, these immune cells are essential targets for the cell-specific delivery of corticosteroids, and their encapsulation in liposomes has been shown to increase their delivery to macrophages (Hu et al., 2019; Sang et al., 2021).

Successful pulmonary delivery of a drug involves a good understanding of the physicochemical characteristics of the delivery system, such as particle size, surface charge, mucopenetration properties, drug loading, cell targeting ability, and cell toxicity (Yıldız-Peköz and Ehrhardt, 2020). Based on the above, we report the development and assessment of three surface-modified drug delivery systems for treating inflammatory lung diseases in this work. Three Dex-loaded liposomes containing PEG and/or HA (Lip-PEG-Dex; Lip-PEG-HA-Dex and Lip-HA-Dex) were designed to cross the mucus layer, reach the lower airways and release Dex within the target cells (Japiassu et al., 2022). We carefully characterized the different Dex-platforms and evaluated their efficacy in *in vitro* and *in vivo* lung inflammation models.

2. Materials and methods

2.1. Materials

Phospholipids 1,2-dihexadecanoyl-sn-glycero-3-phosphocholine (DPPC), 1,2-dipalmitoyl-sn-glycero-3-phosphoethanolamine (DPPE) and 1,2-distearoyl-sn-glycero-3-phosphoethanolamine-N-[methoxy (polyethyleneglycol) -2000](ammonium salt) (PEG) were purchased from Lipoid GmbH (Germany). Cholesterol (CHOL), ethyl (dimethylaminopropyl) carbodiimide (EDC), N-Hydroxysuccinimide (NHS), tert butanol, lipopolysaccharides from *Escherichia coli* O127:B8 (LPS), collagenase type IV (C4-BIOC) and DNase I (10104159001) were obtained from Sigma-Aldrich (France). Hyaluronic acid (400 KDa) was purchased from Contipro (Italy). Dexamethasone (Dex) was purchased from Interchim (France). Water was purified using a MilliQ[®] Reference system from Merck-Millipore (France). The spin labels 5- and 16-doxy-stearic acid methyl ester (5- and 16-DSM) were purchased from Sigma-Aldrich (St. Louis, USA). Solvents were of HPLC analytical grade and were provided by Carlo Erba (Italy). TNF-alpha Mouse Uncoated ELISA Kit and the following monoclonal antibodies were acquired from Thermo Fisher (USA): Anti-Mo F4/80 (clone BM8); anti-Ly-6G (clone 1A8); anti-CD170/Siglec-F (clone 1RNM44N); anti-CD11b (clone M1/70). Antibody anti-mouse CD16/CD32 (clone 2.4G2, Mouse BD Fc Block[™]) was obtained from BD Biosciences (USA).

2.2. Preparation of Dex-loaded liposomes

Lip-PEG-Dex, Lip-PEG-HA-Dex, and Lip-HA-Dex formulations were prepared by a solvent injection method (Japiassu et al., 2022). For Lip-PEG-Dex formulation, DPPC, Chol, mPEG-DSPE in the molar ratio 65:30:5 (40 mg), and dexamethasone (4, 8, or 20 mg) were dissolved in 1 mL of absolute ethanol and stirred for 10 min at 43 °C. The organic solution was injected at a 1.3 mL.min⁻¹ rate into 10 mL of MilliQ[®] water with an automatic

injector. For Lip-PEG-HA-Dex the amount of mPEG-DSPE was reduced from 5% to 2.5% molar ratio, and all the lipids (40 mg) and the Dex (4 mg) were solubilized in *t* butanol/water mixture (60:40 *v/v*). Finally, for Lip-HA-Dex the same solvent mixture and proportions were kept similar to the PEG-HA-Dex's formulation while all mPEG-DSPE was replaced by HA-DPPE conjugate. Once the solvent injection method completed, the liposomes were purified by 2 centrifugation steps. First, an ultracentrifugation (72500 x g) was performed for 4 h at 4 °C to remove any free lipids present in the supernatant. The liposomes, present in the pellet, were then resuspended and centrifuged for 30 minutes at 1700 x g. After this second centrifugation, the liposomes were present in the supernatant, while the nonencapsulated Dex precipitated and was removed by discarding the pellet.

2.3. *Characterization of liposomes*

Liposome size, polydispersity index (PdI) and zeta potential were analyzed by dynamic light scattering (DLS) using a Nano ZS (Malvern Instruments, UK). Liposome suspensions were diluted 10 times either in MilliQ[®] water for size measurements or in 1 mM NaCl for zeta potential measurements. DLS measurements were carried out in triplicates of 10 consecutive runs.

The amount of Dex encapsulated within the liposomes was evaluated by a modified HPLC technique (N'Guessan et al., 2017). Briefly, liposomes containing the drug or standard solutions (0.5 µg/mL to 20 µg/mL) were dissolved in the mobile phase (acetonitrile: water 45:55 *v/v*). Subsequently, samples were vortexed and filtered using 200 nm PTFE filters for precipitate removal. The resulting clear solution was analyzed and quantified using an HPLC-DAD following an isocratic profile.

To assess the impact of the nebulization process, empty liposomes were instilled through a mouse aerosolizer (Penn-Century, USA) into a vial. The size, polydispersity index

(PdI) and zeta potential of the nebulized liposomes were analyzed by DLS as described above and compared to non-nebulized ones.

2.4. EPR spectroscopy

To perform EPR spectroscopy 1 μL of spin markers diluted in ethanol at 5 mg/mL was added to the liposome membranes by placing the liposome solution in contact with a film containing the markers. The labeled liposome suspensions were introduced in capillary tubes sealed by flame. The EPR spectra were recorded using a Bruker EMX spectrometer (Rheinstetten, Germany) operating in the X-band (approximately 9.4 GHz). The instrumental parameters were the following: microwave power, 2 mW; modulation frequency, 100 kHz; amplitude of modulation, 1 G; magnetic field scan, 100 G; scan time, 168 s, and detection time constant, 41 ms, with all measurements performed at room temperature. The best-fit EPR spectra were obtained using the nonlinear least-squares (NLLS) software developed by Freed JH *et al.* (Budil *et al.*, 1996). The best-fit process has as output, among other parameters, the rate of rotational Brownian diffusion, R_{bar} . The motion parameter τ_c , i.e., the rotational correlation time, was obtained via the following equation (Berliner, 1976):

$$\tau_c = \frac{1}{6R_{\text{bar}}} \quad (1),$$

The best-fit spectra were calculated using a model that combines two spectral membrane components as described by Mendanha and Alonso (Mendanha *et al.*, 2018; Mendanha and Alonso, 2015). Each one of these components were simulated using the input parameters for the magnetic tensors g and A : $g_{xx}(1) = 2.0080$; $g_{yy}(1) = 2.0060$; $g_{zz}(1) = 2.0017$; $A_{xx}(1) = 6.9$; $A_{yy}(1) = 6.0$; $A_{zz}(1) = 32.0$; $g_{xx}(2) = 2.0082$; $g_{yy}(2) = 2.0062$; $g_{zz}(2) = 2.0027$; $A_{xx}(2) = 5.7$; $A_{yy}(2) = 5.6$; and $A_{zz}(2) = 31.0$; where the numbers (1) and (2) refer to the first and second spectral component, respectively. The mean rotational correlation time was

calculated as $\tau_c = (N_1 * \tau_{c1} + N_2 * \tau_{c2}) / (N_1 + N_2)$, where N_1 and N_2 are the relative populations of spin labels present in component 1 and 2, respectively, provided by the NLLS software.

2.5. *In vitro cell exposure to Dex*

RAW 264.7 macrophages were seeded onto 12-well culture plates at 5×10^5 cells per 1 mL of culture medium and activated with 50 ng/mL of IFN- γ + 100 ng/mL of LPS for 24 hours. Activated macrophages (M1) were then incubated for 6, 24, or 48 h with Dex-loaded liposomes to obtain a final Dex concentration of 10 μ g/mL. Controls included non-activated macrophages (M0) and M1 macrophages incubated with free Dex at 10 μ g/mL. After incubation, the supernatant was recovered and frozen at -20 °C for further determination of TNF- α concentration by ELISA.

2.6. *Lung inflammation model*

In vivo experimental procedures using C57BL/6J mice were approved by the C2EA - 26 Ethics Committee in Animal Experimentation of IRCIV, under the protocol APAFIS#27142-2020091114373465. Experiments were conducted following the European guidelines (86/609/EEC and 2010/63/EU) and the Principles of Laboratory Animal Care and national French regulations on animal testing (Decree No. 2013-118 of February 1, 2013). C57BL/6J male mice aged 7–12 weeks old were purchased from Janvier Labs, France, and acclimated for at least one week before the experiments. Animals were kept under climate-controlled conditions with a 12 h light/dark cycle, constant temperature (19–22 °C), controlled relative humidity (45–65%), and food and water *ad libitum*.

Acute LPS-induced lung inflammation was obtained by following a similar protocol as applied by Knapp *et al.* (Knapp *et al.*, 2006). The mice were first anesthetized by intraperitoneal (i.p.) injection of a ketamine/xylazine mixture (100 and

10 mg/kg, respectively), and monitored until the disappearance of the pedal reflex. Using a 200 μ L pipette, 15 μ L of an LPS solution (2 mg/mL) was administered twice to the mice, by nasal administration (1.2 μ L of LPS solution/g of mouse weight, i.e. 2.4 mg/kg). The mice were placed on their backs and made to inhale the solution through the nostrils. Subsequently, the mice were allowed to wake up and were monitored daily until euthanized.

After 24 h of LPS stimulation, mice were anesthetized and treated with Dex-loaded liposomes (Lip-PEG-Dex, Lip-PEG-HA-Dex, or Lip-HA-Dex) or free Dex. A fixed Dex dose of 120 μ g/kg from each formulation and control was instilled into the mice lungs through a mouse aerosolizer (Penn-Century, USA). After 6 h of treatment, animals were euthanized using an i.p. overdose of pentobarbital (180 mg/kg). After death was confirmed, the trachea was exposed through an incision and cannulated with a 22-gauge catheter (BD Biosciences). A bronchoalveolar lavage fluid (BALF) volume of 0.3 mL was recovered, and the TNF- α level was quantified using a TNF-alpha Mouse Uncoated ELISA Kit (Invitrogen, ThermoFisher, USA Cat #88-7324) according to the manufacturer's instructions. Subsequently, bronchoalveolar lavage was performed 7 consecutive times by flushing the lungs with 0.6 mL cold PBS to recover the BALF. The first lavage (0.3 mL) was centrifuged at 400 x g for 10 min. The supernatant was kept for TNF- α quantification by ELISA. At the same time, the cellular pellets were pooled with the cells obtained from the subsequent lavages for flow cytometry analysis using an Attune NxT[®] flow cytometer (Thermo Fisher Scientific, USA) and analyzed using FlowJo software (Tree Star).

2.7. Statistical analysis

Statistical differences between groups were evaluated using one-way ANOVA analysis followed by a Turkey's test for multiple comparisons. All values are shown as

mean \pm standard error of the mean (SD). All statistical analyses were performed using GraphPad Prism 6 (GraphPad Software). A p value < 0.05 was considered statistically significant.

3. Results and Discussion

Corticosteroids exert their anti-inflammatory and immunosuppressive activity by interfering with different steps of immune system regulation (Lu et al., 2020). Their mechanism of action is multifactorial, resulting in prostaglandin synthesis and inhibition of cyclooxygenases 1 and 2 (Pandolfi et al., 2019). Due to their anti-inflammatory properties, corticosteroids such as Dex have been prescribed for treating respiratory diseases like COPD and infected SARS patients with severe lung conditions. Corticosteroid regimens aim to reduce the inflammatory process associated with exacerbated cytokine production, pulmonary edema and alveolar damage, which can reduce hypoxia and avoid respiratory failure (Ponzoni et al., 2018; Noreen et al., 2021). Also, cell-mediated responses can be indirectly inhibited by suppressing the production of some interleukins and cytokines, including TNF- α (Kelly et al., 2011). In this work, we designed surface-modified liposomes encapsulating Dex to enhance the drug delivery efficacy across the lung mucus barrier. Three Dex-loaded platforms were developed with different PEG and/or HA mucopenetrating lipid coating (Lip-PEG-Dex; Lip-PEG-HA-Dex and Lip-HA-Dex) and tested for their ability to target AM and to reduce proinflammatory cytokine secretion in lung diseases.

3.1 Physical characterization

The first step of the study was to identify the optimal drug/lipid ratio and maximize the Dex loading efficiency inside the liposome formulations. As Lip-PEG-HA was the most complex formulation of the three, it was used as a model to optimize the formulation

process. Various Lip-PEG-HA were produced using different amounts of Dex (4, 8, and 20 mg) while keeping a fixed (40 mg) total amount of lipids. Results displayed in Table 1 show that all liposomes were monodisperse with an average diameter below 150 nm. However, when 8 and 20 mg of Dex were added to the formulation, the total amount encapsulated did not increase, indicating a saturation of drug incorporation into the lipid bilayer at a drug loading of about 1.5 w/w% (Tsotas et al., 2007). Based on these results, the subsequent formulations were prepared with a 4 mg/40 mg drug/lipid ratio for *in vitro* and *in vivo* tests.

Table 1: Mean diameter, PDI, molar ratio lipid and Dex (mg) encapsulation efficiency (EE%) and calculated Dex encapsulation of Lip-PEG-HA-Dex with different added Dex concentrations. $n=3$.

Lip-PEG-HA (mg added Dex for 40 mg of lipids)	Mean diameter (nm)	ζ potential (mV)	PdI	EE(%)	Dex ($\mu\text{g/mL}$)	Drug loading (drug/lipid w/w%)
4 mg	136 \pm 4	-33 \pm 2	0.19 \pm 0.01	17 \pm 2	70 \pm 4	1.6
8 mg	122 \pm 7	-32 \pm 6	0.21 \pm 0.02	8 \pm 1	68 \pm 3	1.5
20 mg	116 \pm 6	-28 \pm 4	0.23 \pm 0.01	4 \pm 3	71 \pm 7	1.6

The following step was to formulate Dex-loaded liposomes with different surface moieties. Two formulations incorporated PEGylated lipid to reduce unspecific binding with mucus (Lip-PEG and Lip-PEG-HA). In this application a PEG chain with an average size of 2000 Da was chosen as it shows a preferential balance between mucopenetration/ *in vivo* lung retention, and macrophage interaction compared to smaller (750 Da) and larger (5000/10000 Da) ones (Li et al., 2021). HA was also introduced in specific formulations (Lip-PEG-HA and Lip-HA) for its capacity of targeting CD44 receptors and uptake by improving CD44 expressing macrophages.

Table 2: Mean diameter, PdI, ζ Potential, encapsulation efficiency (EE%), Dex concentration and drug loading of Lip-PEG-Dex, Lip-PEG-HA-Dex and Lip-HA-Dex. $n=3$.

Liposome	Mean Diameter (nm)	PdI	Z Potential (mV)	EE(%)	Dex ($\mu\text{g/mL}$)	Drug loading (drug/lipid w/w%)
Lip-PEG-Dex	111 \pm 9	0.16 \pm 0.01	-27 \pm 1	33 \pm 3	135 \pm 8	3.0
Lip-PEG-HA-Dex	136 \pm 4	0.19 \pm 0.01	-33 \pm 2	17 \pm 2	70 \pm 4	1.6
Lip-HA-Dex	189 \pm 6	0.17 \pm 0.02	-40 \pm 1	19 \pm 2	77 \pm 9	1.7

Despite their different surface moieties, all formulations were negatively charged and monodispersed, with mean diameters below 200 nm and PdI values between 0.1 and 0.2 (Table 2). All formulations were stable in storage conditions for at least 3 weeks (Figure 2). Additionally, the high shear stresses of the inhaler/nebulization process did not appear to modify the characteristics of the liposomes (Table 3).

Drug loading was determined to be 3% (drug/lipid w/w%) for Lip-PEG-Dex, 1.6% for Lip-PEG-HA-Dex and 1.7% for Lip-HA-Dex (Table 2). This difference in drug encapsulation is most likely related to the addition of DPPE-HA in the liposome bilayer, which presumably sterically decreases the accommodation of Dex (Modi and Anderson, 2013). This drug loading appears to be on the lower scale, with most of the physically trapped active molecules in liposomes having been characterized by a loading efficiency between 0.1 and 10% (Gómez-Gaete et al., 2007). For non-potent molecules, this modest loading is a drawback that severely hinders the translation from research to clinic. However, for potent drugs, such as corticosteroids, low concentrations are enough to promote an anti-inflammatory effect (Kelly et al., 2011; Samuel et al., 2017). For instance, Lorscheider *et al.* (Lorscheider et al., 2019) demonstrated that 1 $\mu\text{g/mL}$ of Dex, encapsulated in lipid nanoparticles, strongly and significantly reduced inflammatory cytokines in LPS-activated macrophages *in vitro*.

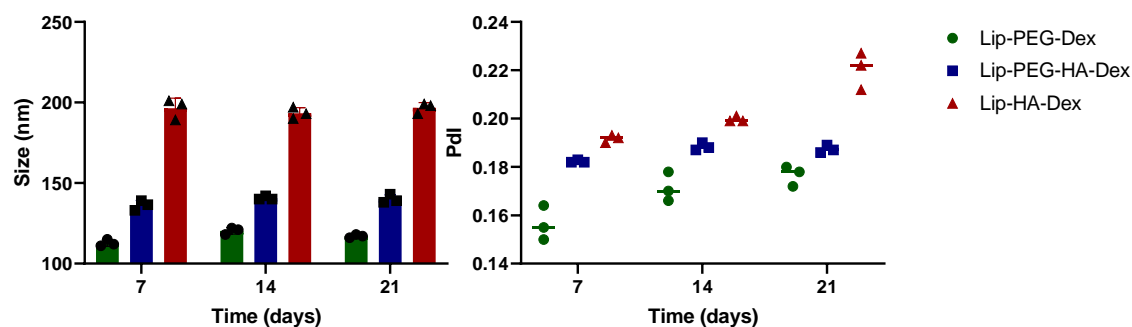


Figure 2: Liposome stability over 3 weeks upon storage at 4 °C. Average diameter (left) and PDI (right) of Lip-PEG-Dex, Lip-PEG-HA-Dex, and Lip-HA-Dex were evaluated. $n=3$.

Table 3: Mean diameter, PDI and ζ Potential of Lip-PEG, Lip-PEG-HA and Lip-HA before and after nebulization. $n=3$ for nebulization.

Liposome	Mean Diameter (nm) before	Mean Diameter (nm) after	PdI before	PdI after	ζ Potential (mV) before	ζ Potential (mV) after
Lip-PEG	129 ± 2	130 ± 2	0.25 ± 0.02	0.18 ± 0.02	-38 ± 1	-37 ± 2
Lip-PEG-HA	93 ± 2	96 ± 3	0.17 ± 0.01	0.18 ± 0.03	-32 ± 1	-27 ± 4
Lip-HA	175 ± 1	165 ± 3	0.14 ± 0.01	0.14 ± 0.02	-42 ± 4	-32 ± 2

To further characterize the individual biophysical features of the lipid platforms and the interaction of the Dex with the different lipids, a spin label approach was used to investigate the dynamic and structural changes induced by the addition of HA-DPPE conjugate, PEG, and Dex within the nanoparticle structures (Mendanha and Alonso, 2015). For this study 5-DSM and 16-DSM lipid spin probes were used, with a nitroxide group attached at different positions in their acyl chains. The influence of Dex incorporation on the dynamics of the lipid bilayers was evaluated and the effect of surface functionalization with HA and PEG (Figure 3). By having the nitroxide group attached to the fifth carbon of its lipid chain, the 5-DSM spin label monitors changes at the hydrophobic/hydrophilic bilayer interface. The 16-DSM spin probe, which has the nitroxide radical placed at the

sixteenth carbon of its acyl chain, is mainly sensitive to changes in the hydrophobic core of the membrane. Through the spectra best-fit, we obtained the motion parameter, i.e., the rotational correlation time, τ_c , used as a measure of the bilayer molecular dynamics. High values of τ_c typically indicate a restricted molecular motion of the spin probes, which characterize a more rigid lipid bilayer (Mendanha et al., 2018; Mendanha and Alonso, 2015). The values obtained for the rotational correlation time (Figure 3-A) reveal that adding Dex in the lipid bilayers led to an enhancement of the 5-DSM dynamics (spectrum b). In contrast, incorporating cholesterol (Chol) promoted rigidity, also indicated by a modification in the low field lineshape (spectrum c). Interestingly, both Chol and Dex must be structured into the liposome membrane near the hydrophobic/hydrophilic bilayer interface since the combined addition of two molecules led to an intermediate 5-DMS dynamics (spectrum d). In addition, no substantial alterations were monitored by the 16-DSM spin label, indicating that Dex did not induce fluidity in the membrane hydrophobic core (Figure 3-B). Figure 3-A also shows that even after individual PEG or HA surface modification (spectra e and g), the liposomes still present a similar dynamic spectrum (c), which characterizes rigid bilayers due to Chol content. This structural stability can be associated with a decrease in burst release, ensuring selective drug delivery to the target cells. By contrast, Lip-PEG-HA presented an increased molecular motion on the membrane polar interface that we explain by the PEG-HA spatial conformation. It was reported²³ that when in dense concentrations, PEG molecules adopt a brush conformation, while low PEG clustering is associated with the mushroom configuration. In sample (f), the PEG mushroom clusters spatially interacted with HA chains, changing the lipid packing on the hydrophobic/hydrophilic bilayer interface, which can be observed through the decrease in the τ_c value.

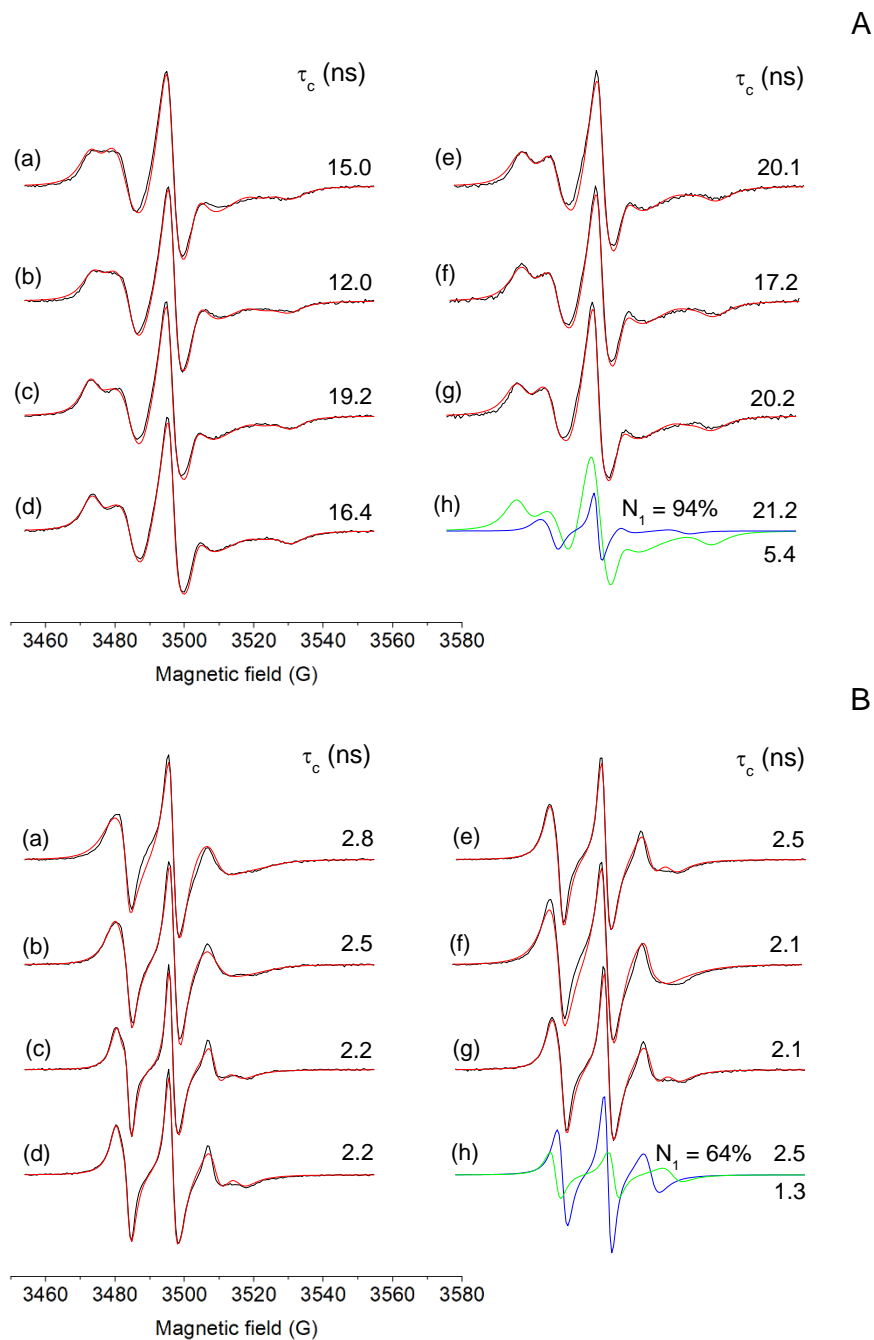


Figure 3-A-B: Experimental (black line) and best-fit (red line) EPR spectra of the spin labels 5-DSM (Panel A) and 16-DSM (Panel B) structured into lipid platforms membranes. The values of the rotational correlation time (τ_c) are indicated for each spectrum. The intensities of the experimental spectra (on the y-axis) are normalized, and the total magnetic field range is 100 G. (a) Lip-DPPC; (b) Lip-DPPC-Dex; (c) Lip-DPPC-Chol; (d) Lip-

DPPC-Dex-Chol; (e) Lip-PEG-Dex; (f) Lip-PEG-HA-Dex; (g) Lip-HA-Dex and (h) deconvoluted spectral components of Lip-HA-Dex, green line = immobilized component (1) and blue line = less immobilized component (2). N_1 represents the fraction of spin probes at the green immobilized component used to compute final τ_c values.

Finally, as expected, the surface modifications did not induce any molecular changes in the membrane core, as seen in Figure 3-B (e)-(g). Altogether, these results indicate that the lipid bilayer matrixes of the different liposomes are compatible with Dex addition and PEG-HA surface modifications while maintaining their structural stability and preventing the undesirable release of the drug content necessary for *in vitro* and *in vivo* efficacy.

3.2. *In vitro* and *in vivo* evaluation

Next, the anti-inflammatory efficacy of the three different Dex-loaded liposome formulations (Lip-PEG-Dex, Lip-PEG-HA-Dex and Lip-HA-Dex) was measured *in vitro* using an established IFN- γ /LPS-inflammation model (Knapp et al., 2006). LPS-activated M1 macrophages were treated with either free Dex or Dex-loaded liposomes for 6, 24, or 48 h, and their secretion of TNF- α was quantified by ELISA and compared to non-activated M0 macrophages (Figure 4). TNF- α was chosen as a readout for our *in vitro* and *in vivo* experiments as it can be produced by activated macrophages, lymphocytes or monocytes (Kim et al., 2021). The main stimulus for its production is the presence of LPS, which composes the membrane of gram-negative bacteria. After being produced and released, TNF- α binds specifically to TNF receptors (TNF-R) I and II for its biological effects (Lowry, 1993). When released in low concentrations, TNF- α acts on endothelial cells, promoting vasodilation and stimulating the secretion of chemokines. Also, it has been shown to play a crucial role in orchestrating the cytokine cascade in many inflammatory diseases (Malaviya et al., 2017). Thus, because of its role as a "master regulator" of

inflammatory cytokine production, it has been proposed as a key targeted biomarker in multiple inflammatory diseases (Hiremath et al., 2020; Lowry, 1993; Thomson et al., 2012).

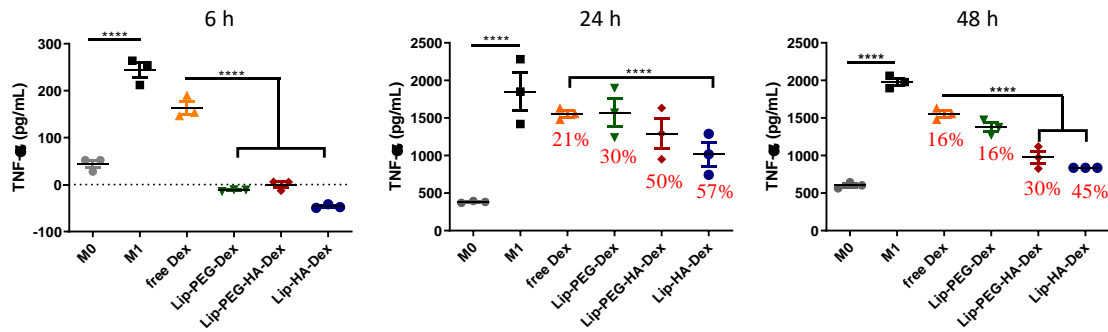


Figure 4: Effect of the treatment with free Dex (orange), Lip-PEG-Dex (green), Lip-PEG-HA-Dex (red) and Lip-HA-Dex (blue) on TFN- α release by M0 (grey) and M1 (black) LPS-activated macrophages. The final concentration of Dex was 10 μ g/mL. (A) TFN- α quantification at 6 h after treatment; (B) TFN- α quantification at 24 h after treatment; (C) TFN- α quantification at 48 h after treatment. Data are represented as mean \pm SD, **** p <0.0001 analyzed by one-way ANOVA test followed by Tukey's multiple comparison test. PBS: Phosphate buffered saline; LPS: lipopolysaccharide; M0: non-activated macrophage; M1: proinflammatory macrophage; Lip: liposome; PEG: poly(ethylene glycol); HA: hyaluronic acid; Dex: dexamethasone.

Results presented in Figure 4 show a clear increase in the production of the proinflammatory cytokine by activated (M1) macrophages when compared to M0 macrophages ($p < 0.0001$). While a decrease in TFN- α secretion was observed after treatment with free Dex (21% after 24 h and 16% after 48 h), a significantly higher reduction in TFN- α levels were measured after 24 h of exposure to HA-liposomes (50-57%). This difference between treated cells decreased with time, but Lip-Dex platforms constantly demonstrated better efficacy compared to free Dex. When comparing the level

of TNF- α secreted by activated macrophages after treatment with different Lip-Dex platforms, data in figure 4 show that Lip-HA-Dex has the highest anti-inflammatory activities followed by Lip-PEG-HA-Dex and then by Lip-PEG-Dex. This highest efficacy of HA-bearing formulations is most likely due to the higher internalization rate of the liposomes through HA interaction with CD44 receptors that are known to be overexpressed on the surface of activated macrophages, as demonstrated in an earlier study (Japiassu et al., 2022). Additionally, adding PEG molecules on the surface of liposomes has been shown to reduce the efficacy of this CD44 targeting and may explain how Lip-PEG-HA-Dex appeared to be less effective than Lip-HA-Dex.

The three Dex-loaded liposomes were then tested *in vivo* using an established LPS-induced lung inflammation model (Japiassu et al., 2022). Data presented in Figure 5 showed that nasal LPS challenge led to an increased concentration of TNF- α in BALF, indicating an inflammatory response. As expected, the treatment with free Dex reduced TNF- α concentration by 45% compared to untreated animals but with high inter-animal variability. Comparatively, using Lip-Dex improved efficiency in reducing TNF- α secretion, with Lip-PEG-Dex, Lip-PEG-HA-Dex, and Lip-HA-Dex liposomes-based treatment leading to a TNF- α secretion reduction of respectively 68, 60 and 64%.

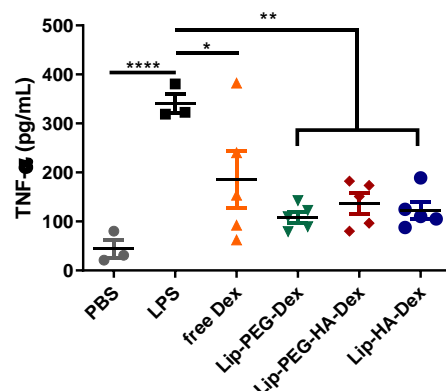


Figure 5: Effect of TNF- α release in BALF after 6 h of treatment with free Dex (orange), Lip-PEG-Dex (green), Lip-PEG-HA-Dex (red) or Lip-HA-Dex (blue). Final concentration

of Dex was 120 $\mu\text{g}/\text{kg}$. Lines and error bars show the mean and SD, respectively. **** $p < 0.0001$; ** $p < 0.001$; * $p < 0.05$ analyzed by one-way ANOVA test followed by Tukey's multiple comparisons test. Dots represent individual animals. PBS: Phosphate buffered saline.

Interestingly, this decrease in TNF- α BALF concentration was more consistent across animals treated with Lip-Dex compared to free Dex. This demonstrates that Dex encapsulation in liposomes can increase its therapeutic efficacy and pharmacodynamics parameters [42]. These findings are in agreement with the *in vitro* results and indicate the ability of Lip-Dex platforms to overcome lung barriers and contribute to consistent lung distribution and retention. However, unlike *in vitro* data (figure 4), no significant differences were found between the three Dex lipid platforms in reducing TNF- α levels. This disparity reveals the difference between *in vitro* and *in vivo assays* and the necessity of preclinical animal experiments. Interestingly, the cell population remains unchanged when studying BALF's cellular composition after 6 h of treatment with free Dex or Lip-Dex (Figure 6). This indicates that our strategy affects cell activity and inflammation but does not disrupt the overall cell composition, which is key to fighting any underlying infections.

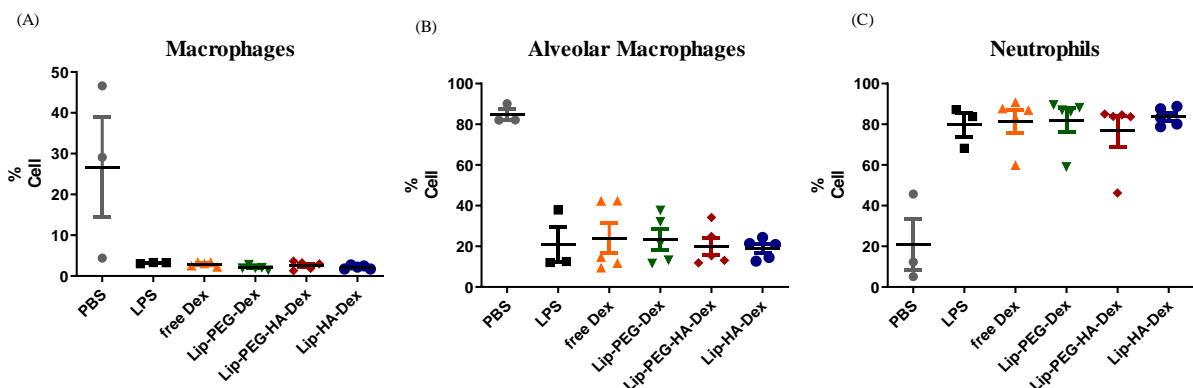


Figure 6: *In vivo* cell profile analyzed in (A) Macrophages (B) Alveolar macrophages and (C) Neutrophils by flow cytometry after 6 hours of treatment with free Dex and Lip-Dex,

The animals were treated with 120 µg/kg of Dex.

4. Conclusion

In this paper, we demonstrated that the encapsulation of Dex into targeted liposomes is feasible and can be considered a new therapeutic option for inflammatory pulmonary diseases. However, it is important to notice that the addition of DPPE-HA has a detrimental effect on the drug encapsulation rate. We also demonstrated that TNF- α levels produced by macrophages were efficiently reduced *in vitro* and *in vivo* after treatment with HA and PEG-surface-modified liposomes containing Dex. *In vitro* data indicates a more efficient targeting of the HA-bearing liposomes towards activated macrophages. The *in vivo* results are more contrasted, demonstrating that Dex encapsulated within liposomes has a more consistent efficacy but did not reveal any significant difference between the three lipid platforms. Future perspectives of this work will need to focus on chronic treatment at a lower dose to clarify the actual effect of liposomes surface modification with HA and PEG on the efficacy of the treatments.

CRedit authorship contribution statement

K.B.J, F.F, N.T and E.F. conceptualized and designed the study. K.B.J., A.M., C.C., Y.L., QW, S.D. and S.A.M. conducted the experiments. F.F. and E.F supervised the research. K.B.J and T.L.N performed statistical analysis. K.B.J, FF, T.L.N., N.T., E.M.L. and E.F. analyzed the data and wrote the manuscript. All authors discussed the progress of research and reviewed the manuscript.

Data availability

Data will be made available on request.

Conflicts of interest

The authors declare no conflicts of interest.

Acknowledgements

KBJ acknowledges a scholarship from Programa de Pós-Graduação em Nanotecnologia Farmacêutica of Federal University of Goiás, a CAPES scholarship from the Doctoral Program Abroad (Process n. 88881.361526/2019-01), also a scholarship from the doctoral school: ED Innovation Thérapeutique – Du Fondamental à l'appliqué [ITFA n. 569], and Institut Galien Paris-Saclay (UMR 8612) of University Paris-Saclay. The authors acknowledge the Région Ile-de-France for financial support of the IPSIT platforms.

Formatting of funding sources

This work was funded by the Brazilian agency Coordenação de Aperfeiçoamento de Pessoal de Nível Superior (CAPES) and Centre National de la Recherche Scientifique (CNRS UMR 8612). Authors acknowledge financial support from ANR (ANR JCJC NANOSEPSIS FF) and EuroNanomed III (ARROWNANO 2017-1892 EF). EF and FF is a part of the FHU SEPSIS (Saclay and Paris Seine Nord Endeavour to Personalize Interventions for Sepsis).

References

- Almeida, A.P.B., Damaceno, G.B.R., Carneiro, A.F., Bohr, A., Gonçalves, H.R., Valadares, M.C., Nascimento, T.L., Lima, E.M., 2019. Mucopenetrating lipoplexes modified with PEG and hyaluronic acid for CD44-targeted local siRNA delivery to the lungs. *J. Biomater. Appl.* 34, 617–630.
<https://doi.org/10.1177/0885328219863291>
- Blank, F., Fytianos, K., Seydoux, E., Rodriguez-Lorenzo, L., Petri-Fink, A., Garnier, C., Rothen-Rutishauser, B., 2017. Interaction of biomedical nanoparticles with the pulmonary immune system. *J. Nanobiotechnology* 15, 1–9.
<https://doi.org/10.1186/s12951-016-0242-5>

- Budil, D.E., Sanghyuk, L., Saxena, S., Freed, J.H., 1996. Nonlinear-Least-Squares Analysis of Slow-Motion EPR Spectra in One and Two Dimensions Using a Modified Levenberg–Marquardt Algorithm. *J. Magn. Reson. Ser. A* 120, 155–189. <https://doi.org/10.1006/JMRA.1996.0113>
- Daley-Yates, P.T., 2015. Inhaled corticosteroids: potency, dose equivalence and therapeutic index. *Br. J. Clin. Pharmacol.* 80, 372–380. <https://doi.org/https://doi.org/10.1111/bcp.12637>
- García-Fernández, A., Sancho, M., Bisbal, V., Amorós, P., Marcos, M.D., Orzáez, M., Sancenón, F., Martínez-Mañez, R., 2021. Targeted-lung delivery of dexamethasone using gated mesoporous silica nanoparticles. A new therapeutic approach for acute lung injury treatment. *J. Control. Release* 337, 14–26. <https://doi.org/10.1016/J.JCONREL.2021.07.010>
- Gómez-Gaete, C., Tsapis, N., Besnard, M., Bochot, A., Fattal, E., 2007. Encapsulation of dexamethasone into biodegradable polymeric nanoparticles. *Int. J. Pharm.* 331, 153–159. <https://doi.org/10.1016/j.ijpharm.2006.11.028>
- Hiremath, J., Renu, S., Tabynov, K., Renukaradhya, G.J., 2020. Pulmonary inflammatory response to influenza virus infection in pigs is regulated by DAP12 and macrophage M1 and M2 phenotypes. *Cell. Immunol.* 352, 104078. <https://doi.org/10.1016/j.cellimm.2020.104078>
- Hu, G., Guo, M., Xu, J., Wu, F., Fan, J., Huang, Q., Yang, G., Lv, Z., Wang, X., Jin, Y., 2019. Nanoparticles targeting macrophages as potential clinical therapeutic agents against cancer and inflammation. *Front. Immunol.* 10, 1998. <https://doi.org/10.3389/FIMMU.2019.01998/BIBTEX>
- Japiassu, K.B., Fay, F., Marengo, A., Louaguenouni, Y., Cailleau, C., Denis, S., Chapron, D., Tsapis, N., Nascimento, T.L., Lima, E.M., Fattal, E., 2022. Interplay

- between mucus mobility and alveolar macrophage targeting of surface-modified liposomes. *J. Control. Release* 352, 15–24.
<https://doi.org/10.1016/j.jconrel.2022.10.006>
- Kelly, C., Jefferies, C., Cryan, S.-A., 2011. Targeted Liposomal Drug Delivery to Monocytes and Macrophages. *J. Drug Deliv.* 2011, 1–11.
<https://doi.org/10.1155/2011/727241>
- Kim, Y., Park, E.J., Kim, T.W., Na, D.H., 2021. Recent progress in drug release testing methods of biopolymeric particulate system. *Pharmaceutics* 13, 1–23.
<https://doi.org/10.3390/pharmaceutics13081313>
- Knapp, S., Florquin, S., Golenbock, D.T., van der Poll, T., 2006. Pulmonary Lipopolysaccharide (LPS)-Binding Protein Inhibits the LPS-Induced Lung Inflammation In Vivo. *J. Immunol.* 176, 3189–3195.
<https://doi.org/10.4049/jimmunol.176.5.3189>
- Lai, S.K., Wang, Y.Y., Wirtz, D., Hanes, J., 2009. Micro- and macrorheology of mucus. *Adv. Drug Deliv. Rev.* 61, 86. <https://doi.org/10.1016/J.ADDR.2008.09.012>
- Li J, Zheng H, Xu EY, Moehwald M, Chen L, Zhang X, Mao S. Inhalable PLGA microspheres: Tunable lung retention and systemic exposure via polyethylene glycol modification. *Acta Biomater.* 2021 Mar 15;123:325-334. doi: 10.1016/j.actbio.2020.12.061. Epub 2021 Jan 14. PMID: 33454386
- Lorscheider, M., Tsapis, N., Ur-Rehman, M., Gaudin, F., Stolfa, I., Abreu, S., Mura, S., Chaminade, P., Espeli, M., Fattal, E., 2019. Dexamethasone palmitate nanoparticles: An efficient treatment for rheumatoid arthritis. *J. Control. Release* 296, 179–189. <https://doi.org/10.1016/j.jconrel.2019.01.015>
- Lowry, S.F., 1993. Tumor Necrosis Factor and Other Cytokines as Mediators of Clinical Sepsis. *Host Def. Dysfunct. Trauma, Shock Sepsis* 253–261.

https://doi.org/10.1007/978-3-642-77405-8_27

Lu, C., Xiao, Y., Liu, Y., Sun, F., Qiu, Y., Mu, H., Duan, J., 2020. Hyaluronic acid-based levofloxacin nanomicelles for nitric oxide-triggered drug delivery to treat bacterial infections. *Carbohydr. Polym.* 229, 115479.

<https://doi.org/10.1016/j.carbpol.2019.115479>

Malaviya, R., Laskin, J.D., Laskin, D.L., 2017. Anti-TNF α therapy in inflammatory lung diseases. *Pharmacol. Ther.* <https://doi.org/10.1016/j.pharmthera.2017.06.008>

Matthieu, B., Matthieu, J., Nicolas, G., Patrice, G., Srine, M., William, C., Olivier, M., 2014. Comparison of intrapulmonary and systemic pharmacokinetics of colistin methanesulfonate (CMS) and colistin after aerosol delivery and intravenous administration of CMS in critically ill patients. *Antimicrob. Agents Chemother.* 58, 7331–7339. <https://doi.org/10.1128/AAC.03510-14>

McDonough, A.K., Curtis, J.R., Saag, K.G., 2008. The epidemiology of glucocorticoid-associated adverse events. *Curr. Opin. Rheumatol.* 20, 131–137.

<https://doi.org/10.1097/BOR.0b013e3282f51031>

Mendanha, S.A., Alonso, A., 2015. Effects of terpenes on fluidity and lipid extraction in phospholipid membranes. *Biophys. Chem.* 198, 45–54.

<https://doi.org/10.1016/J.BPC.2015.02.001>

Mendanha, S.A., dos Anjos, J.L.V., Maione-Silva, L., Silva, H.C.B., Lima, E.M., Alonso, A., 2018. An EPR spin probe study of the interactions between PC liposomes and stratum corneum membranes. *Int. J. Pharm.* 545, 93–100.

<https://doi.org/10.1016/J.IJPHARM.2018.04.057>

Modi, S., Anderson, B.D., 2013. Bilayer composition, temperature, speciation effects and the role of bilayer chain ordering on partitioning of dexamethasone and its 21-phosphate. *Pharm. Res.* 30, 3154–3169. <https://doi.org/10.1007/s11095-013-1143->

- N'Guessan, A., Fattal, E., Chapron, D., Gueutin, C., Koffi, A., Tsapis, N., 2018. Dexamethasone palmitate large porous particles: A controlled release formulation for lung delivery of corticosteroids. *Eur. J. Pharm. Sci.* 113, 185–192. <https://doi.org/10.1016/j.ejps.2017.09.013>
- Noreen, S., Maqbool, I., Madni, A., 2021. Dexamethasone: Therapeutic potential, risks, and future projection during COVID-19 pandemic. *Eur. J. Pharmacol.* 894, 173854. <https://doi.org/10.1016/J.EJPHAR.2021.173854>
- Pandolfi, L., Frangipane, V., Bocca, C., Marengo, A., Genta, E.T., Bozzini, S., Morosini, M., D'Amato, M., Vitulo, S., Monti, M., Comolli, G., Scupoli, M.T., Fattal, E., Arpicco, S., Meloni, F., 2019. Hyaluronic acid-decorated liposomes as innovative targeted delivery system for lung fibrotic cells. *Molecules* 24, 3291. <https://doi.org/10.3390/molecules24183291>
- Ponzoni, M., Pastorino, F., Di Paolo, D., Perri, P., Brignole, C., 2018. Targeting macrophages as a potential therapeutic intervention: Impact on inflammatory diseases and cancer. *Int. J. Mol. Sci.* 19, 1953. <https://doi.org/10.3390/ijms19071953>
- Rhen, T., Cidlowski, J.A., 2005. Antiinflammatory Action of Glucocorticoids — New Mechanisms for Old Drugs. *N. Engl. J. Med.* 353, 1711–1723. <https://doi.org/10.1056/nejmra050541>
- Saag, K.G., 1997. Low-dose corticosteroid therapy in rheumatoid arthritis: Balancing the evidence. *Am. J. Med.* 103, S31–S39. [https://doi.org/10.1016/S0002-9343\(97\)90006-1](https://doi.org/10.1016/S0002-9343(97)90006-1)
- Saag, K.G., Koehnke, R., Caldwell, J.R., Brasington, R., Burmeister, L.F., Zimmerman, B., Kohler, J. a, Furst, D.E., 1994. Low dose long-term corticosteroid therapy in

- rheumatoid arthritis: an analysis of serious adverse events. *Am. J. Med.* 96, 115–23. [https://doi.org/10.1016/0002-9343\(94\)90131-7](https://doi.org/10.1016/0002-9343(94)90131-7)
- Samuel, S., Nguyen, T., Choi, H.A., 2017. Pharmacologic Characteristics of Corticosteroids. *J Neurocrit Care* 10, 53–59. <https://doi.org/10.18700/jnc.170035>
- Sang, X., Wang, Y., Xue, Z., Qi, D., Fan, G., Tian, F., Zhu, Y., Yang, J., 2021. Macrophage-Targeted Lung Delivery of Dexamethasone Improves Pulmonary Fibrosis Therapy via Regulating the Immune Microenvironment. *Front. Immunol.* 12, 393. <https://doi.org/10.3389/FIMMU.2021.613907/BIBTEX>
- Schneider, C.S., Xu, Q., Boylan, N.J., Chisholm, J., Tang, B.C., Schuster, B.S., Henning, A., Ensign, L.M., Lee, E., Adstamongkonkul, P., Simons, B.W., Wang, S.-Y.S., Gong, X., Yu, T., Boyle, M.P., Suk, J.S., Hanes, J., 2017. Nanoparticles that do not adhere to mucus provide uniform and long-lasting drug delivery to airways following inhalation. *Sci. Adv.* 3, e1601556. <https://doi.org/10.1126/sciadv.1601556>
- Suk, J.S., Xu, Q., Kim, N., Hanes, J., Ensign, L.M., 2016. PEGylation as a strategy for improving nanoparticle-based drug and gene delivery. *Adv. Drug Deliv. Rev.* 99, 28–51. <https://doi.org/10.1016/j.addr.2015.09.012>
- Thomson, E.M., Williams, A., Yauk, C.L., Vincent, R., 2012. Overexpression of Tumor Necrosis Factor- α in the Lungs Alters Immune Response, Matrix Remodeling, and Repair and Maintenance Pathways. *Am. J. Pathol.* 180, 1413–1430. <https://doi.org/10.1016/J.AJPATH.2011.12.020>
- Tsotas, V.-A., Mourtas, S., Antimisiaris, S.G., 2007. Dexamethasone incorporating liposomes: effect of lipid composition on drug trapping efficiency and vesicle stability. *Drug Deliv.* 14, 441–5. <https://doi.org/10.1080/10717540701603530>
- Wang, Y.Y., Lai, S.K., Suk, J.S., Pace, A., Cone, R., Hanes, J., 2008. Addressing the

PEG Mucoadhesivity Paradox to Engineer Nanoparticles that “Slip” through the Human Mucus Barrier. *Angew. Chem. Int. Ed. Engl.* 47, 9726–9729.

<https://doi.org/10.1002/ANIE.200803526>

World Health Organization, 2021. WHO model list of essential medicines - 22nd list, 2021. Tech. Doc. 2021.

Yıldız-Peköz, A., Ehrhardt, C., 2020. Advances in Pulmonary Drug Delivery.

Pharmaceutics 12, 1–7. <https://doi.org/10.3390/PHARMACEUTICS12100911>

